Int. J. Electrochem. Sci., 10 **(2015)** 5001 - 5012

International Journal of
ELECTROCHEMICAL
SCIENCE
www.electrochemsci.org

Graphite Anodes Activated by Melamine, Carbamide, $ZnCl_2$ and H_3PO_4 in Microbial Fuel Cells

Junjing Qiao[1], *Peter GIRGUIS*[2,*], *Dongmei LI*[1], *Jingxing MA*[3], *Lankun CAI*[1], *Lehua ZHANG*[1,2,*]

[1] State Environmental Protection Key Laboratory of Environmental Assessment and Control on Chemical Process, School of Resources and Environmental Engineering, East China University of Science and Technology, Shanghai, 200237, China
[2] Department of organismic and evolutionary biology, Harvard University, 16 Divinity Avenue, Room 3085, Cambridge, MA 02138, USA
[3] Department of Water Pollution Control (STEP), Universite Libre de Bruxelles. Boulevard du Triomphe, Campus Plaine - CP 208, B-1050 Brussels, Belgium.
[*]E-mail: lezhanghua@ecust.edu.cn

Received: 27 January 2015 / *Accepted:* 18 March 2015 / *Published:* 28 April 2015

Here we evaluated the graphite anodes activated by melamine, carbamide, $ZnCl_2$ and H_3PO_4 in microbial fuel cells (MFCs). Results indicated that the graphite activated by melamine, carbamide and zinc chloride, respectively, could improve the voltage output and power densities, as well as decrease the internal resistances. MFCs with graphite activated by melamine as anode achieved the highest maximum power generation ($0.442W/m^3$), 26.8% greater than the untreated graphite. The reason for improved performance is the introduction of nitrogen-containing functional groups on the electrode that can increase the efficiency of electron transfer from the bacteria to the anode surface, enhance surface wettability and improve bacterial adhesion. The chemical activation processes are the most cost-effective because of simply immersion, no heating, no electrochemical process and no expensive chemicals.

Keywords: Microbial fuel cells (MFCs), Graphite, Activation, Surface functional groups, Surface wettability

1. INTRODUCTION

Microbial fuel cells (MFCs) are the promising bio-electrochemical reactors that use the catalysis of microorganisms to recover electrical energy from wastewater, as well as to simultaneously remove organics in wastewaters [1, 2]. The MFC anode is the site of current deposition, from adhered bacterial biofilms, planktonic bacteria capable of shuttling electrons via soluble mediators, as well as

the abiotic oxidation organic matter. The performance of the anode as an electron acceptor has been shown to play an important, overall role in MFC power production [3, 4].

It has been suggested that MFC performance could be effectively improved by modification enhancing bacterial adhesion and decreasing the interfacial electron transfer resistance. To date, several studies have focused on modifying the electrode surfaces in order to enable more efficient anode materials for power generation. Diffusion of metals and metal oxides into carbon-based electrodes, such as Mn^{4+}/ Mn^{2+}+Ni^{2+}, Fe_3O_4/Fe_3O_4+Ni^{2+}, Pt and tungsten carbide, has been demonstrated to be effective in enhancing MFC power generation [3-8]. Non-metal modification of carbon-based electrodes, including the addition of conductive polymers [9-13], neutral red and ammonia [14, 15], also showed a positive impact on power performance. Indeed, Cheng *et al*. used an ammonia-treated carbon cloth as an anode in a single-chamber air-cathode MFC to increase power density [15]. Logan conducted additional tests to confirm the treatment of the brush electrodes with ammonia gas was an effective method of reducing the acclimation time and increasing power, while power production of the MFCs with the treated anode was 37 % higher than that with the untreated brush anodes [16]. Saito et al. used carbon cloth anodes modified with 4(N,N-dimethylamino) benzene diazonium tetrafluoroborate to increase nitrogen-containing functional groups at the anode surface and found that this power density was 24% greater than an untreated anode, similar to that obtained with an ammonia gas treatment previously [17]. To found an inexpensive flat electrodes for use in MFCs, Wang et al. developed the pretreatment processes of carbon mesh and found that heating the carbon mesh in a muffle furnace (450 ° C for 30 min) resulted in a maximum power density of 922 mW/m^2 with this heat-treated anode, which was 7% less than that achieved with carbon cloth treated by a high temperature ammonia gas process (988 mW/m^2) [18]. To develop a less energy-intensive method, Feng *et al*. examined three different treatment methods, including acid soaking in a solution of ammonium peroxydisulfate, heating at 450° C and a combination of both processes, the results shown that the combined heat and acid treatment improve power production to 1370mW/m^2, which is 34% larger than the untreated control and that the power increases are related to higher N/C ratios and a lower C–O composition on the anode surface [19]. Zhu *et al*. modified an activated carbon fiber felt with nitric acid and ethylenediamine as anodes in MFCs, which shortened the start-up time and increased the power output [20]. Tamon *et al*. [21] found that the surface area and micropore volume decreased while the adsorption sites increased in the carbon because of the activation by HNO_3.

Chemical activation has proven to be a lower-cost, effective and common-used method to improve the surface characteristics of the carbon material by altering the specific surface area, as well as the species and quantity of surface functionality, and thus changing the adsorption characteristics and electrochemical performances of the electrode materials, especially for graphite and carbon. Chemical activators modifying the carbon materials can be classified into three kinds by their activation mechanism: oxidants (e.g.HNO_3, H_3PO_4, O_3 and H_2O_2), reducing agents (e.g. ammonia, carbamide and melamine formaldehyde) and neutral chemicals (e.g. steam and $ZnCl_2$) [22, 23]. We chose to test the widely available, lower cost materials that are highly relevant when considering scale-up in future industrial applications. The aims of this study are primarily to improve the anode performance, electrical conductivity and bacterial adhesion by chemical activation, which could lead to increases in power production in MFCs. To this end, we conducted a series of treatments,

characterized anode and MFC performance, and further examined the surface characteristics of chemically activated graphite to demonstrate the effect on power production.

2. MATERIALS AND METHODS

2.1 Chemical activation

Graphite rods (length of 13 cm, diameter of 6 mm, Shanghai Xinxia Mechanical and Electrical Material Co. Ltd., China) were used as the graphite electrodes in the tests, and were washed with deionized water for 15 minutes, then air-dried for 1 hour at 25±2 ºC. Pre-washed graphite rods were immersed for 36 h at 25±2 ºC in 85%(wt) H_3PO_4 (P), 80 g/L $ZnCl_2$ solution (Zn), saturated carbamide solution (U) and 80 g/L melamine formaldehyde solution (M), respectively. Finally, the chemically activated graphite rods, as well as the untreated ones (B), were washed by deionized water and air-dried for 3 hours. Both the chemically activated rods and the untreated controls were used as the anodic materials to evaluate the performances of the MFCs (described below).

2.2 Chemically activated and untreated graphite used as the anodic materials in MFCs

A test tube MFC (TTMFC) system (see Pham, *et al.* [24]) was used for these experiments. In this system (Figure 1), a polytetrafluoroethylene (PTFE) tube with 20 mL volume was used as the anode chamber. The bottom end of the tube was sealed with a $1cm^2$ circular proton exchange membrane (0.083 S/cm, 0.89 meq/g, Nafion 117, DuPont Co., Delaware, USA). The membrane ends of the TTMFCs were submerged into a 50 mM potassium hexacyanoferrate solution and contacted with a graphite-felt electrode serving as the cathode. The top end was capped tightly and supported a chemically activated or untreated graphite rod (length of 13 cm, diameter of 6 mm). Four graphite rods in each tube were connected through wires to external resistance that closed the circuit with the cathode to become a multi-MFC system. In the external circuit, a variable-resistance box (ZX21, 0.1-99999.9 Ω, Shanghai Precision and Scientific Instrument Co. Ltd., Shanghai, China) setting 10000 Ω was connected in series. The output voltage was continuously recorded with the data acquisition (RBH 8223h, Beijing Ruibohua Control Technology Co., Ltd. China).

The anodic medium (50 mM phosphate buffer solution of pH 7.2 with 0.5 g NH_4Cl, 0.1 g $MgSO_4$, 0.1 g $CaCl_2 \cdot 2H_2O$, 0.1 g KCl, 1 g $NaHCO_3$ and 1 mL trace element solution) [25] was supplemented with 1 g sodium acetate per liter. The anodic inoculum was taken from another MFC operating for ~ 10 months in our laboratory [26]. The inoculum was flushed with N_2 for 60 mins, and then 18 mL was injected into each tube. Five groups of multi-MFC systems (H_3PO_4: P-MFC; $ZnCl_2$: Zn-MFC; carbamide solution: U-MFC; melamine formaldehyde solution: M-MFC and untreated ones: B-MFC) were processed to measure the performance of MFCs using the chemically activated or untreated graphite rods as anodic materials.

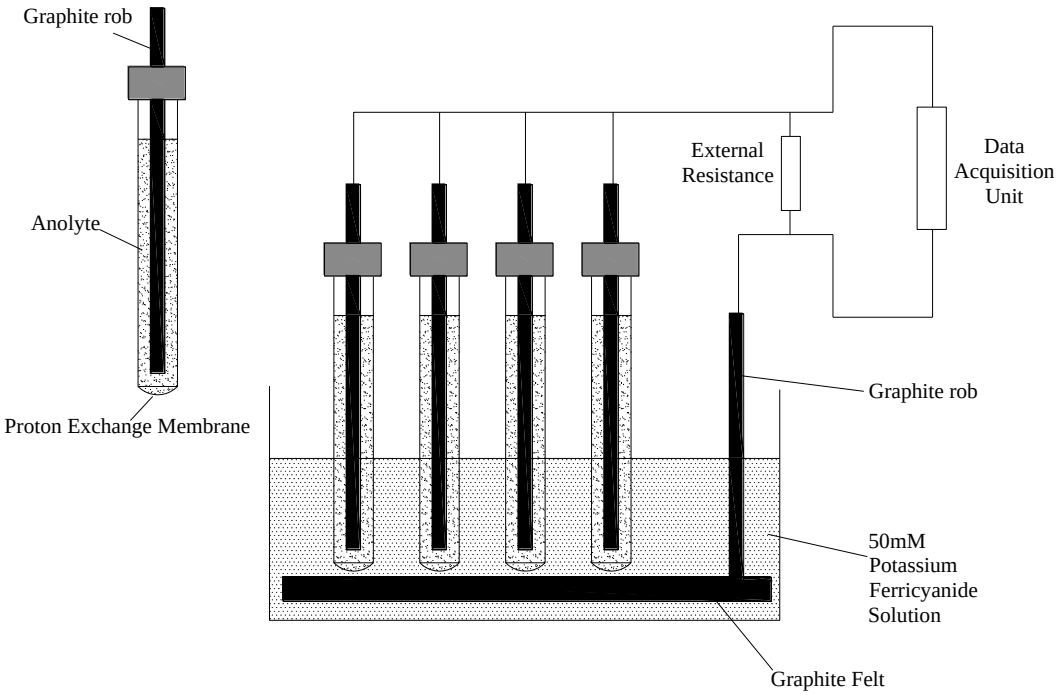

Figure 1. Schematic of a test tube MFC (TTMFC) system.

Polarization studies were carried out by varying the external resistances from 30000 Ω to 1000 Ω. The voltage (E) across an external resistor (R_{ext}) was measured and recorded by the data acquisition unit every 15 mins. The current (I) was calculated according to Ohm's law as

$$I = \frac{E}{R_{ext}} \quad (1)$$

and power density was calculated as in Logan et al.[1]

$$P = \frac{E \times I}{V_{Anode}} = \frac{E^2}{R_{ext} \times V_{Anode}} \quad (2)$$

where P is the volumetric power (W/m^3), V_{Anode} is the anodic compartment volume of MFC reactor. Internal resistance of the MFCs was measured based on the slope of line from the plot of voltage versus current [27].

2.3 Surface characteristics of activated and untreated graphite

The activated and untreated graphite were rinsed with deionized water and stored at between 25 ° C to 30 ° C for 48 h prior to analysis. The methylene blue test was used to predict the specific surface area of the activated and untreated graphite [22]. Fourier transform infrared spectroscopy (FTIR) [29, 30] was carried out by using a Nicolet 5700 (Nicolet Instrument Co. Ltd., U.S.A.). Spectra were collected from 350 cm^{-1} to 7800 cm^{-1} with a resolution of 0.9 cm^{-1} and a scan rate of 65 s^{-1}. The FTIR experiments were performed on the powdered samples, with KBr addition. The elemental analysis of

the activated and untreated graphite was taken by a scanning electron microscopy with a falconenergy-dispersive X-ray spectroscope (SEM-EDS) (S-4800, Hitachi Science System Ltd., Japan). Water contact angle and diiodomethane contact angle on chemically activated graphite were measured using a Contact Angle Meter (JC2000D3, Shanghai Zhongchen Co. Ltd., China). The measurements of surface wettability were carried out at a temperature of 26 ^{o}C and a humidity of 0.26.

3. RESULTS AND DISCUSSION

3.1 Polarization curves of MFCs

Figure 2 shows the polarization curves of MFCs with the activated or untreated graphite anodes. The results indicated that the voltage output of MFCs with the graphite anodes activated by ZnCl2, carbamide and melamine increased, in contrast to the MFCs with untreated anode. The voltage output of M-MFC with a graphite anode activated by melamine was the highest. In contrast, the P-MFC with a graphite anode activated by H_3PO_4 showed an even lower voltage than that of the untreated control (B-MFC). The open cell voltages of Zn-MFC, U-MFC, M-MFC and B-MFC were 680, 603, 638 and 579 mV while the open cell voltage of P-MFC was less than 400 mV. The linear fits of polarization curves in Zn-MFC, U-MFC, M-MFC and B-MFC were carried out and the internal resistances in MFCs were calculated by the slope of the fitted line. The internal resistances in Zn-MFC, U-MFC, M-MFC and B-MFC were 12188.9, 11955.6, 11460.0 and 13213.3 Ω. According to the results of the linear-fitting, the internal resistances in U-MFC and M-MFC were much lower than that in B-MFC.

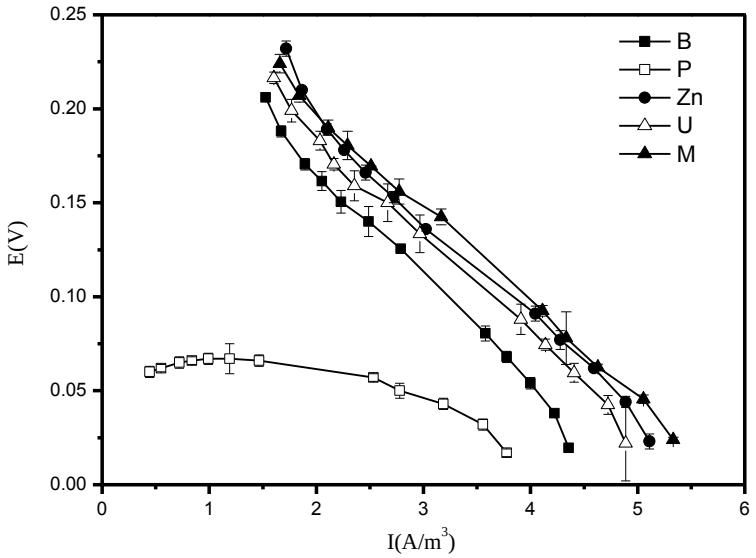

Figure 2. Polarization curves of of the MFCs with the anodic material using the untreated graphite electrode (B), the electrode chemically activated by H_3PO_4 (P), $ZnCl_2$ (Zn), carbamide (U) and cyanurotriamide (M), respectively.

3.2 Power generation of MFCs

Figure 3 shows the power density curves of MFCs with the chemically activated or untreated graphite anodes. The power density of P-MFC decreased significantly while the power densities of Zn-MFC, U-MFC and M-MFC increased, when compared to the B-MFC (see figure 3). The Zn-MFC, U-MFC and M-MFC achieved the maximum power density of 0.415 W/m^3, 0.401 W/m^3 and 0.442 W/m^3, which increased by 19.1%, 15.0% and 26.8%, respectively. Notably, while the M-MFC achieved the highest maximum power density, the maximum power density of P-MFC was the lowest of 0.144 W/m^3, which decreased by 58.7%.

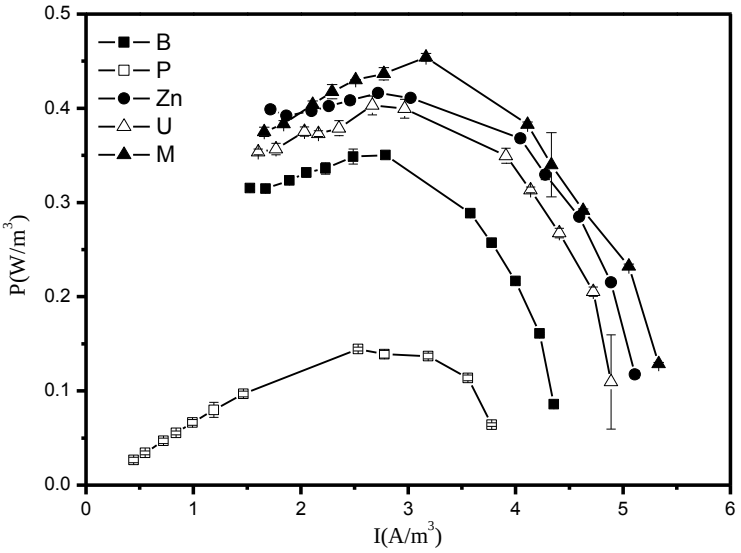

Figure 3. Power density curve of the MFCs with the anodic material using the untreated graphite electrode (B), the electrode chemically activated by H_3PO_4 (P), $ZnCl_2$ (Zn), carbamide (U) and cyanurotriamide (M), respectively.

3.3 Surface characteristics of graphite

Previous studies suggest that the increase of the specific surface area of an electrode in MFCs plays an important role in the improvement of process performance [17]. In the data presented here, the methylene blue derived from the activated electrodes was 2.57, 3.78, 2.59 and 3.60 mg/g for $ZnCl_2$, H_3PO_4, carbamide and melamine respectively. The methylene blue derived of the untreated graphite anodes was 2.49 mg/g. The results indicated that graphite chemically activated by H_3PO_4 and melamine could increase the specific surface area significantly, though only slight improvements were observed in those chemically activated by $ZnCl_2$ and carbamide,.

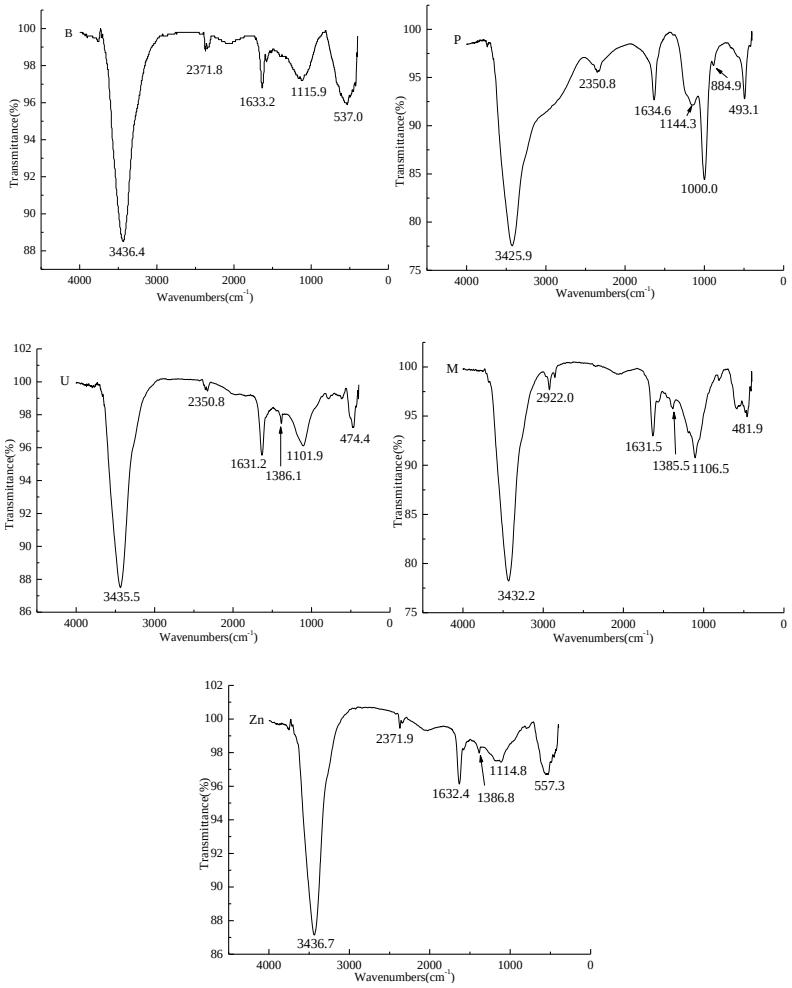

Figure 4. The FTIR spectra of the untreated graphite (B) and the graphite chemically activated by H_3PO_4 (P), $ZnCl_2$ (Zn), carbamide (U) and cyanurotriamide (M), respectively.

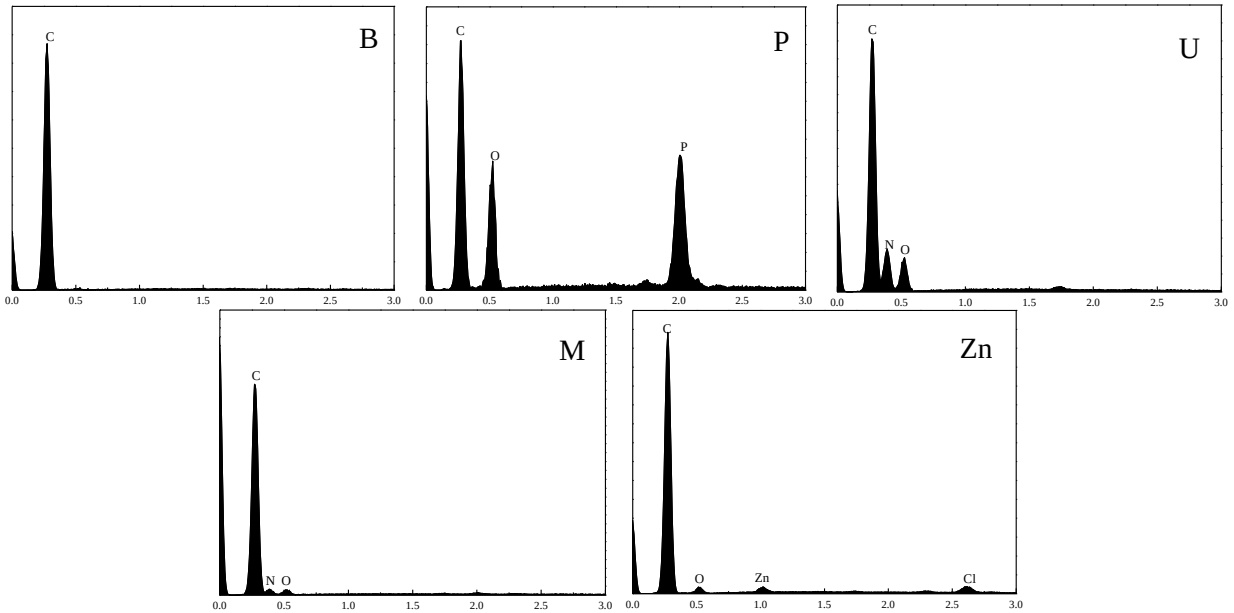

Figure 5. EDS analysis based on the SEM (×500) of the untreated graphite (B) and the graphite activated by H_3PO_4 (P), $ZnCl_2$ (Zn), carbamide (U) and cyanurotriamide (M), respectively.

FTIR analysis was performed to study the surface functional groups on the activated and untreated graphite, (see Figure 4). As shown, the group of hydroxyl (-OH) stretching bands was at the bands of around 3430 cm^{-1}, while the bands around 1635 cm^{-1} were assigned to the group of carbonyl (-C=O). Also, the intensities of the bands in these two ranges strengthened on the surface of graphite activated by H_3PO_4 and melamine, which suggested the increased loading of carboxyl, hydroxyl and carbonyl. Besides, two additional peaks at 1000 cm^{-1} and 1144 cm^{-1} occurred with the graphite activated by H_3PO_4, which are attributed to P-O-C, P-OH, and P=O groups, respectively. Moreover, in the case of graphite activated by carbamide and melamine, an additional peak at 1105 cm^{-1} was observed, which was related to the presence of C-N bonds. Graphite activated by melamine introduced the stretching band peaks of CH_2 at 2853 cm^{-1} and 2922 cm^{-1}.

Table 1. Water contact angle and diiodomethane contact angle on chemically activated and untreated graphite. B: untreated ones; P: H_3PO_4; U: carbamide solution; Zn: $ZnCl_2$; M: melamine formaldehyde solution.

		B	P	U	M	Zn
Water Contact Angle	1	88.4	53.68	101	65.47	71.55
	2	89.51	51.73	90.99	76.13	67.7
	3	104.9	60.1	79.22	76.73	76.27
	4	96.73	58.49	90.97	72.54	69.87
	5	95.91	55.63	103	71.15	75.31
	Average	95.09±4.91	55.93±2.70	93.04±7.17	72.40±3.27	72.14±2.92
CH_2I_2 Contact Angle	1	26.81	54.07	34.75	32.92	35.83
	2	21.01	53.13	29.89	39.39	32.27
	3	23.77	54.1	27.94	34.29	35.71
	4	22.15	53.13	33.37	30.97	36.86
	5	26.48	54.77	31.12	36.67	33.24
	Average	24.04±2.08	53.84±0.57	31.41±2.12	34.85±2.55	34.78±1.62

The results of the SEM-EDS analysis of the graphite untreated and activated by H_3PO_4, $ZnCl_2$, carbamide, as well as melamine, are shown in Figure 5. The results of EDS analyses indicated that, in addition to carbon, there was measureable oxygen, phosphorus, nitrogen and zinc, which varied in abundance among the treatments. Carbon, oxygen and phosphorus were the other three dominant elements observed on the surface of the graphite activated by H_3PO_4. Moreover, oxygen and nitrogen were observed on the surface of the graphite activated by carbamide (Figure 5U) and melamine (Figure 5M), though with much smaller fractions. For the graphite activated by $ZnCl_2$ (Figure 5Zn), the zinc and chlorine were negligible. The chemically activated graphite had clearly been supplemented with additional surface functional groups after chemical activation, which indicates consistent results with FTIR analysis. Notably, Cheng, *et al*. [15] reported that the presence of nitrogen-containing functional groups at the surface could improve the electron flow to the anode surface. On the surface of the graphite activated by carbamide or melamine, the nitrogen-containing functional groups were introduced according to the analysis of FTIR and EDS, while they improved the performances of U-

MFC and M-MFC. The increment of oxygen functional groups and phosphorus-containing functional groups increased the electron transfer resistances and thus, reduced the efficiency of electron transfer on the surface of graphite activated by H_3PO_4, which consequently reduced the performance of P-MFC.

The contact angle (see table 1) was measured to analyze surface wettability. The results showed that the contact angles of graphite activated by H_3PO_4, $ZnCl_2$ and melamine have decreased significantly, which showed the enhancement of the surface wettability. However, the impact of activation by carbamide on surface wettability was negligible. Dai, *et al* [26] reported that the bacterial adhesion was increased with the surface wettability. It could be the reason why the performance of Zn-MFC and M-MFC were enhanced comparing to that of B-MFC.

3.4 Impact on the anodic performance by the surface characteristics

The graphite activated by $ZnCl_2$, carbamide and melamine used as the anode in MFCs could improve the performances of MFCs (see table 2). Moreover, melamine is suggested to be the best choice among all these five chemical activation materials in this research because of the increased specific surface area and surface wettability, as well as the introduction of nitrogen-containing functional groups, which improved the performance of M-MFC. The increasing specific surface area and surface wettability improved but the introduction of oxygen-containing functional groups worsen the performance of P-MFC; the introduction of nitrogen-containing functional groups improved but the decreasing surface wettability worsen the performance of U-MFC; the increasing surface wettability improved the performance of Zn-MFC but there is on the introduction of nitrogen-containing functional groups and there is only a slightly impact of activation by $ZnCl_2$ on specific surface area. Cheng, *et al*. [15] and Valerie, *et al*. [32] reported that the nitrogen-containing functional groups at the graphite surface could increase because of the activation by ammonia vapors. In this research, the activation by melamine increased the nitrogen-containing functional groups at the graphite surface, too. However, activation process by melamine is more simple and cost-effective due to the simply immersion and no heating. H_3PO_4 is a moderately strong acid with a light oxidation potential. Chen, *et al.* [33] reported that too much acidic surface functional groups were detrimental for microbial activity in MFCs due to the inhibiting effect of H^+, which was consistent with our result.

Table 2. Impact on the performance of microbial fuel cells (MFCs) by the surface characteristics including the specific surface area, nitrogen-containing functional groups, oxygen-containing functional groups and surface wettability of activated and untreated graphites.

	B-MFC	P-MFC	U-MFC	M-MFC	Zn-MFC
Specific surface area	0	+1	0	+1	0
Nitrogen-containing functional groups	0	0	+1	+1	0
Oxygen-containing functional groups	0	-1	0	0	0
Surface wettability	0	+1	-1	+1	+1
Total	0	+1	0	+3	+1

0: The impact on performance of MFCs was negligible. +1: The impact on performance of MFCs was positive. -1: The impact on performance of MFCs was negative.

However, Zhou, *et al.* [34] reported that the electrochemical oxidation in nitric acid benefited to the microbial attachment and electron transfer on the anode surface, which might contribute to the performance improvement of the MFCs. Here, the graphite was only simply immersed into H_3PO_4 or HNO_3 without electrochemical oxidation.

3.5 Practical implications

Graphite and carbon should be commonly used as anodic materials when MFCs are scaled up in future industrial applications. The surface characteristics of graphite and carbon chasing from the market are unknown because of the raw materials and technological process. A huge challenge is that graphite and carbon chasing from the market is not suitable to be used as anodic materials. Diffusion of metals and metal oxides into carbon-based materials is expensive because of their complicated technological process, such as electrochemical process or pyrolysis process (when manganese or iron are used), as well as because of the price of metals (when platinum, nickel or cobalt are used) [3-8]. Non-metal modification of carbon-based electrodes, including the addition of conductive polymers, [9-13] Neutral Red and ammonia [14, 15], is also expensive because of their complicated technological process as well as the price of chemicals. Chemical activation processes reported here are the most cost-effective (simply immersion, no heating, no electrochemical process, no expensive chemicals) and on site treatment technologies. Workers would modify the surface characteristics of graphite and carbon on site where the MFCs are built by either sequencing batch or continuous way. The MFCs with the activated or unactivated graphite anodes had been operated in the lab for four months. However, further explore is needed to investigate the stability of these modification in a long term operation.

3.6 Chemical activation mechanism

Oxidation-reduction reactions play an important role in improving the surface characteristics by chemical activation when oxidants (e.g.HNO_3, H_3PO_4, O_3 and H_2O_2), reducing agents (e.g. ammonia, carbamide and melamine formaldehyde) used as chemical activators [23, 24, 31]. The oxidation reactions resulted in the present of oxygen-containing functional groups, such as hydroxyl (-OH), aldehyde (-CHO) and carboxyl (-COOH). The results of FTIR (see Fig. 5) showed that the group of hydroxyl (-OH) and carbonyl (-C=O) were strengthened on the surface of graphite activated by H_3PO_4, which suggested the increased loading of oxygen-containing functional groups. The results of SEM-EDS (see Fig. 5) showed that oxygen was one of the dominant elements observed on the surface of the graphite activated by H_3PO_4. The reduction reactions resulted in the present of nitrogen-containing functional groups, such as amino (-NH_2), secondary amino (-NH-). The results of FTIR (see Fig 4) showed that the C-N bonds were observed in the case of graphite activated by carbamide and melamine. The results of SEM-EDS (see Fig5) showed that nitrogen were observed on the surface of the graphite activated by carbamide (Fig 5U) and melamine (Fig 5M). Besides, substitution reaction or other reactions could also play the role in introducing the more complicated functional groups, such as

P-O-C, P=O groups (see Fig 4 and Fig 5) during the chemical activation processes. Relative intensity of oxidation-reduction reactions would be much lower when neutral chemicals (e.g. steam and $ZnCl_2$) used as chemical activators. There are not oxygen-containing and nitrogen-containing functional groups present in the graphite surface after chemical activation (see Fig 4 and Fig 5).

4. CONCLUSIONS

The graphite activated by melamine, carbamide and zinc chloride, respectively, could improve the voltage output and power densities, as well as decrease the internal resistances. The MFCs with a graphite anode activated by melamine achieved the highest maximum power generation ($0.442W/m^3$), 26.8% greater than the untreated graphite. The introduction of nitrogen-containing functional groups on the surface of activated-by-melamine graphite anode increased the efficiency of electron transfer from the bacteria to the anode surface, enhanced surface wettability and improved bacterial adhesion. The surface characteristics of graphite would be modified on site, where the MFCs are built, using chemical activation processes that are the most cost-effective (simply immersion, no heating, no electrochemical process, no expensive chemicals) when MFCs are scaled up in future industrial applications.

ACKNOWLEDGEMENTS
This work was supported by the National Natural Science Foundation of China (NSFC) (20906026), Shanghai Pujiang Program (09PJ1402900) and the Scientific Research Foundation for the Returned Overseas Chinese Scholars State Education Ministry (B200-C-0904).

References

1. X. Su, Y. Tian, Z. Sun, Y. Lu, and Z. Li, *Biosens. Bioelectron.*, 49(2013) 92-98.
2. Y. Ahn, B.E. Logan, *Appl. Microbiol. Biotechnol.*, 93 (2012)2241-2248.
3. D.H. Park, and J.G. Zeikus, *Biotechnol. Bioeng., 3(2003)348-355.*
4. Y. Fan, S.-K. Han, and H. Liu, *Energy Environ. Sci.*, 5 (2012) 8273-8279.
5. D.A. Lowy, L.M. Tender, G. Zeikus, D.H. Park, R. Derek, and D.R. Lovley, *Biosens. Bioelectron., 21(2006)2058-2063.*
6. D. Prasad, S. Arun, M. Murugesan, S. Padmanaban, R.S. Satyanarayanan, S. Berchmans, and V. Yegnaraman, *Biosens. Bioelectron.*, 22(2007)2604-2610.
7. A. ter Heijnea, H.V.M .Hamelersa, M. Saakesb, and C.J.N. Buisman, *Electrochim. Acta*., 53(2008)5697-5703.
8. N.V. Prabhu, and D. Sangeetha, *Chem. Eng. J.*, 243 (2014) 564-571.
9. H. Shirakawa, E. J. Louis, A.G. MacDiarmid, C.K. Chiang, and A.J. Heeger, *J. Chem. Soc. Chem. Comm.*,16(1977)578-580.
10. Y. Yuan, S.G. Zhou, and L. Zhuang, *J. Power Sources*, 195(2010)3090-3093.
11. C. Li, L.B. Zhang, L.L. Ding, H.Q. Ren, and H. Cui, *Biosens. Bioelectron.*, 26(2011)4169.
12. S. Uwe, N. Juliane, and S. Fritz, *Angew. Chem. Int. Ed.*, 42(2003)2880-2883.
13. Y. J. Zou, C.L. Xiang, L.N. Yang, L.L. Sun, F. Xu, and Z. Cao, *Int. J. Hydrogen Energy.*, 33(2008)4856-4862.

14. D.H. Park, and S.K. Kim, *Biotechnol. Lett., 22(2000)1301-1304.*
15. S.A. Cheng, and B.E. Logan, *Electrochem. Commun.*, 9(2007)492-496.
16. B.E. Logan, S. Cheng, V. Watson, and G. Estadt, *Environ. Sci. Technol.*, 41(2007)3341-3346.
17. T. Saito, M. Mehanna, X. Wang, R.D. Cusick, Y. Feng, M.A. Hickner, and B.E. Logan, *Bioresour. Technol.*, 102(2011)395-398.
18. Y.J. Feng, Q. Yang, X. Wang, and B.E. Logan, *J. Power sources*, 195(2010)1841-1844.
19. X. Wang, S. Cheng, Y.J. Feng, M.D. Merrill, T. Saito, and B.E. Logan, *Environ. Sci. Technol.*, 43(2009)6870-6874.
20. N.W. Zhu, X. Chen, T. Zhang, P.X. Wu, P. Li, and J.H. Wu, *Bioresour. Technol.*, 102(2011)422-426.
21. H. Tamon, and M .Okazaki, *Carbon*, 34(1996)741-746.
22. B. Erable, N. Duteanu, S.M.S. Kumar, Y.J. Feng, M.M. Ghangrekar, and K. Scott, *Electrochem. Commun.*, 11(2009)1547–1549.
23. T. Xu, and X.Q. Liu, *Chinese. J. Chem. Eng.*, 37(2009)70-74.
24. T.H. Pham, N. Boon, and P. Aelterman, *Appl. Microbiol. Biotechnol.*, 77(2008)1119-1129.
25. K .Rabaey, W. Ossieur. M. Verhaege, and W. Verstraete, *Water Sci. Technol.*, 52(2005)515-523.
26. Y.P. Mao, L.H. Zhang, D.M. Li, H.F. Shi, Y.D. Liu, and L.K. Cai, *Electrochim. Acta.*, 55(2011)7804-7808.
27. C. Picioreanua, I.M. Head, K.P. Katuri, M.C.M. Loosdrecht, and K. Scott, *Water Res.*, 41(2007)2921-2940.
28. A. Altamirano-Gutiérrez, O. Jiménez-Sandoval, J. Uribe-Godínez, R.H. Castellanos, E. Borja-Arco, and J.M. Olivares-Ramírez, *Int. J. Hydrogen Energy.*, 34(2009)7983-7994.
29. J. Uribe-Godínez, R.H. Castellanos, E. Borja-Arco, A. Altamirano-Gutiérrez, and O. Jiménez-Sandoval, *J. Power Sources*, 177(2008)286-295.
30. S.L. Dai, X.H. Luo, H.Y. Huang, and Y.M. Deng, *Environ. Poll. Control*, 31(2009)51-53.
31. H. Ago, T. Kugler, F. Cacialli, R.W. Salaneck, S.P.M. Shaffer, H.A. Windle, and H.R. Friend, *J. Phys. Chem. B.*, 103(1999)8116-8121.
32. V. J. Watson, C. N. Delgado, and B. E. Logan, *J. Power Sources*, 242(2013)756-761.
33. Z. H. Chen, K. X. Li , P. Zhang, L.T. Pu, X. Zhang, and Z. Fu, *Chem. Eng. J.*, 259 (2015) 820-826.
34. M. H. Zhou, M. L. Chi, H. Y. Wang, and T. Jin, *Biochem. Eng. J.*, 60 (2012) 151-155.